Rare Metal Materials and Engineering
Volume 49, Issue 3, March 2020
Available online at www.rmme.ac.cn

Science Press

Cite this article as: Rare Metal Materials and Engineering, 2020, 49(3): 0749-0754.

ARTICLE

Dissolution Mechanism and Electrochemical Behavior of CeO_2 in Molten CeF_3-LiF-BaF_2

Li Binchuan[1], **Li Shiju**[2], **Kong Yapeng**[1], **Chen Jianshe**[1], **Liu Kuiren**[1], **Han Qing** [1]

[1] Key Laboratory for Ecological Metallurgy of Multimetallic Mineral (Ministry of Education), Northeastern University, Shenyang 110819, China; [2] Key Laboratory of Electromagnetic Processing of Materials (Ministry of Education), Northeastern University, Shenyang 110819, China

Abstract: The dissolution mechanism of CeO_2 in molten CeF_3-LiF-BaF_2 and the electrochemical behavior of Ce(III) on molybdenum electrode in molten CeF_3-LiF-BaF_2 was investigated. Cyclic voltammetry, chronoamperometry and potentiostatic electrolysis were performed to investigate the reduction mechanism of Ce(III) ions. The products obtained by dissolution reaction and potentiostatic electrolysis were characterized by X-ray diffraction (XRD), scanning electron microscopy (SEM) and energy dispersive spectrometer (EDS). The results show that CeO_2 can dissolve into the fluoride molten salts in the form of CeOF by reacting with CeF_3. Further, cerium oxyfluorides can be directly reduced to cerium metal with a purity of 99.38 wt%~99.81 wt% on molybdenum electrode via a reversible three-electron-transfer process, which is controlled by diffusion.

Key words: cerium; molten fluorides; CeF_3-LiF-BaF_2; CeO_2; electrodeposition

As a kind of abundant rare earth metal, cerium metal is extensively used in special alloys and hydrogen storage materials[1-5]. Particularly, with the new applications in the fields of permanent magnetic materials,[6-8] new energy,[9,10] optics and optoelectronics[11,12], it comes up with higher requirements at purity of cerium metal. Electrochemical preparation methods, i.e. electrowinning and electrorefining, are effective and promising approaches for obtaining high-purity rare earth metals and their alloys.

At present, cerium metal is produced by electrolysis in molten fluoride salts using ceric dioxide as raw material. However, relevant researches on the electrochemical process and mechanism of cerium metal preparation are mainly focused on molten chloride salts. Zhang et al[13] studied the electrochemical behavior of Ce(III) on aluminum electrode in molten LiCl-KCl-$CeCl_3$ salts. The electrode reaction process of Ce(III) on molybdenum electrode in molten electrolyte was investigated by cyclic voltammetry, chronopotentiometry and square wave voltammetry. The results show that Ce(III) ions are electrochemically reduced to cerium via a three-electron reaction and the process is controlled by the diffusion of Ce(III) towards the surface of cathode[14]. Qi [15] et al studied the cathodic process of Ce(III) ions in molten NaCl-CsCl and proposed that the cathodic process includes two steps, i.e. the one-electron-transfer process and the two-electron-transfer process. Furthermore, sporadic studies have reported the electrochemical behavior of Ce(III) in molten fluoride salt. Constantin et al[16] conducted the electrochemical studies on Ce(III) generated by adding CeF_3 in molten LiF-NaF and LiF-NaF-CaF_2 salts. They confirmed that the reduction process involves a three-electron-transfer step and metallic cerium can be deposited as fine powder. The study of electrochemical reduction of Ce(III) in molten LiF-BaF_2 on molybdenum electrode using CeF_3 as solute was performed by cyclic voltammetry and chronopotentiometry. The results shows that the reduction of Ce(III) is a one-step process and controlled by Ce(III) diffusion in melt[17]. However, there are few reports on the cerium preparation by electrolysis in fluoride-oxide molten salts. Using CeO_2 as raw material, the dissolution mechanism of CeO_2 and the electrochemical behavior of Ce(III) in molten CeF_3-LiF-BaF_2 were investigated. The results might provide useful information for the direct extraction and separation of cerium from oxide in molten fluoride salt.

Received date: March 29, 2019

Corresponding author: Han Qing, Ph. D., Professor, School of Metallurgy, Northeastern University, Shenyang 110819, P. R. China, Tel: 0086-24-83686997, E-mail: hanq@smm.neu.edu.cn

1 Experiment

CeF_3 (≥99.9%, Sinopharm Chemical Reagent Co., Ltd), LiF (≥98.0%, Shanghai Aladdin Bio-Chem Technology Co., Ltd) and BaF_2 (≥99.0%, Sinopharm Chemical Reagent Co., Ltd) were used as the components of electrolyte. CeO_2 (≥99.9%, Sinopharm Chemical Reagent Co., Ltd) was used as the additive.

20 g mixed salts (the mass ratios are shown in Table 1) were weighted and placed in a graphite crucible. After drying at 200 °C for 5 h, the mixed salts were heated at 940 °C for 2 h under argon atmosphere (>99.99%, 1 L/min), and finally cooled to room temperature by air-cooling. The melting products were identified by XRD (D/max-2500PC, X'Pert Pro), SEM (JSM-7800F, Ultra Plus) and EDS after grinding.

Electrolysis measurement and constant potential electrolysis experiments were performed in a sealed stainless steel reactor with inlet and outlet gas lines. Argon gas (>99.99%) was injected into the reactor continuously with a flow rate of 1 L/min. The mixture of electrolyte CeF_3-LiF-BaF_2 with a mass ratio of 73:17:10 was contained in a graphite crucible (70 mm in inner diameter, 100 mm in depth) standing in the reactor and dried at 300 °C for 5 h to remove residual water. Subsequently, the temperature was increased and kept at 940 °C. Once the salts were melted, a three-electrode system was used in the constant potential electrolysis experiment. The graphite crucible was used as the electrolytic cell and also functioned as the counter electrode. Graphite rod (spectroscopic pure, 6 mm in diameter) was used as the pseudo-reference electrode. Molybdenum rod (>99.95%, 1.5 mm in diameter, 600 mm in length) was used as the working electrode. The experimental conditions in cyclic voltammetry and chronopotentiometry measurements were similar to those in the constant potential electrolysis experiment. All the electrolysis measurement and constant potential electrolysis experiments were performed using Zahner IM6e electrochemical workstation. After constant potential electrolysis, the obtained products were washed and dried, and finally identified by XRD and SEM. The contents of cerium and impurity in the products were analyzed by Inductively Coupled Plasma (ICP, Optima 8300).

2 Results and Discussion

2.1 Dissolution mechanism of CeO_2 in molten CeF_3-LiF-BaF_2

The electrolysis process of rare earth oxides in molten fluoride salt is similar to the aluminum electrolysis process. Hence, the dissolution behavior of cerium oxide in molten CeF_3-LiF-BaF_2 is important for the electrodeposition process of cerium metal. Xu et al[18] proposed that the possible dissolution reactions of rare earth oxides in molten fluoride salts can be described as follows.

1) Simple dissociation reaction:

$$CeO_2 \rightleftharpoons Ce^{4+} + 2O^{2-} \quad (1)$$

2) CeO_2 reacts with carbon in the form of graphite:

$$2CeO_2 + C \rightleftharpoons 2Ce^{3+} + 3O^{2-} + CO \quad (2)$$

3) CeO_2 reacts with the co-ions in the molten salt, i.e. CeF_3.

In order to determine the dissolution mechanism of CeO_2 in molten CeF_3-LiF-BaF_2, the mixtures of CeO_2 with one or more of CeF_3, LiF and BaF_2 were melted in graphite crucible at 940 °C for 2 h. Table 1 lists the composition and mass of the molten salts and Fig.1 shows the XRD patterns of the melting products.

As shown in Fig.1, the diffraction peaks of product A obtained after melting the mixture of CeF_3 and CeO_2 are identified as CeOF. This suggests that CeO_2 reacts with CeF_3 and forms CeOF, in which the cerium ion is trivalent. The XRD patterns of the products B, C and D obtained by melting the mixtures of CeO_2 and LiF, BaF_2 and LiF-BaF_2 show that the phase composition of the mixtures is changed after melting, indicating that CeO_2 cannot react with LiF, BaF_2 or LiF-BaF_2. Simultaneously, as can be seen from Fig.1, the diffraction peaks of CeOF in product E are observed after melting CeO_2 into molten LiF-BaF_2-CeF_3. In summary, the dissolution of CeO_2 results in the formation of cerium oxyfluorides in molten CeF_3-LiF-BaF_2.

Table 1 Composition and mass ratio of the mixed molten salts

Product No.	Composition	$m(CeO_2)$/g	$m(CeF_3)$/g	m(LiF)/g	$m(BaF_2)$/g
A	CeF_3-CeO_2	9.32	10.68	–	–
B	LiF-CeO_2	17.37	–	2.63	–
C	BaF_2-CeO_2	9.91	–	–	10.09
D	LiF-BaF_2-CeO_2	9.22	–	1.40	9.38
E	CeF_3-LiF-BaF_2-CeO_2	6.04	6.91	0.91	6.14

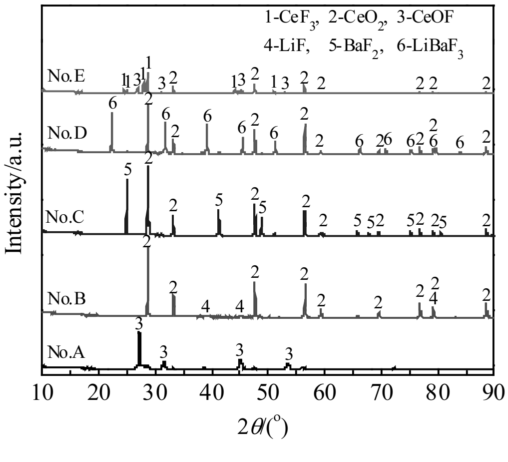

Fig.1 XRD patterns of reaction products labeled in Table 1 after melting at 940 °C for 2 h

Fig.2 shows the SEM image and EDS spectrum of the product obtained after melting the mixture of CeF$_3$ and CeO$_2$. The EDS result shows that the product is mainly composed of cerium, oxygen and fluorine, and the atomic percentage of these three elements is close to 1:1:1. This result is consistent with the observation from XRD. Identical conclusions on the formation of rare earth oxyfluorides have been obtained in relevant studies, such as the electrodeposition of neodymium from LiF-NdF$_3$-Nd$_2$O$_3$[19] and LiF-CaF$_2$-AlF$_{-}$Nd$_2$O$_3$[20].

2.2 Cyclic voltammogram

Fig.3 shows the cyclic voltammograms of molybdenum metal electrodes in molten LiF and LiF-BaF$_2$ salts. As shown in Fig.3a, the cyclic voltammogram of molybdenum metal electrode in molten LiF exhibits no notable current during the cathodic scan until about –1.6 V (vs. C/CO$_x$), where a significant increase in reduction current peak A is observed. The corresponding reoxidation peak A′ emerges upon reversing the potential scan. On the basis of relevant studies on the LiF-based molten electrolytes[20-23], it can be concluded that the A and A′ peaks are attributed to the deposition of Li(I) ions and reoxidation of the deposited metal lithium, respectively.

Fig.3b presents the cyclic voltammogram of the molybdenum metal electrode in molten LiF-BaF$_2$ (mass ratio: 17:73) salts. As shown in the figure, a reduction current peak B forms at about –1.75 V (vs. C/CO$_x$), which can be attributed to the electrochemical deposition of Ba(II).

As the potential continues to shift negatively, the reduction current peak A is observed. Upon reversing the potential scan, reoxidation peak A′ appears together with the peak B′ due to the reoxidation of deposited lithium and barium, respectively.

Fig.4 shows the cyclic voltammogram curve of molybdenum electrode in molten CeF$_3$-LiF-BaF$_2$ (mass ratio: 73:17:10). It can be seen that a reduction current peak C appears at about –1.5 V (vs. C/CO$_x$). Compared with the cyclic voltammetry curves mentioned above, this current peak C can be attributed to the electrochemical deposition of Ce(III), formed by CeF$_3$.

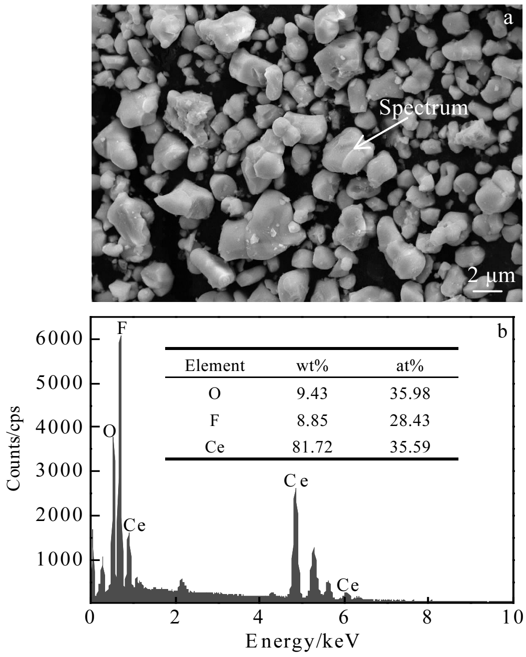

Fig.2 SEM image (a) and EDS spectrum (b) of the product obtained by melting the mixture of CeF$_3$ and CeO$_2$ at 940 °C for 2 h

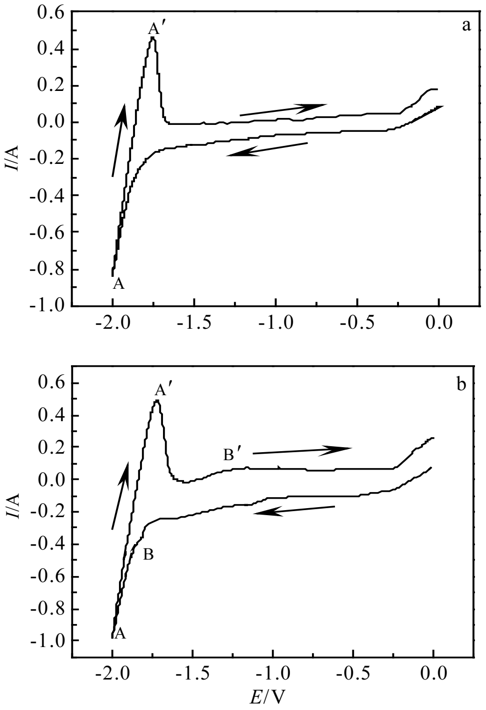

Fig.3 Cyclic voltammetry curves of molybdenum electrode in molten LiF (a) and LiF-BaF$_2$ (b) with a scan rate of 150 mV/s

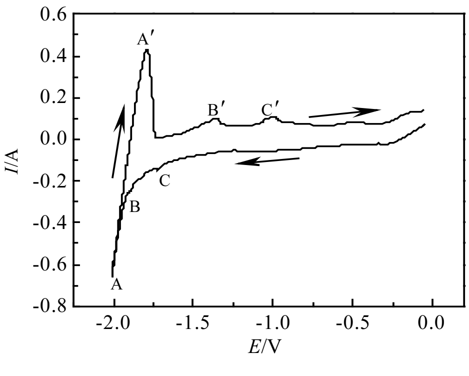

Fig.4 Cyclic voltammetry curve of molybdenum electrode in molten LiF-BaF$_2$-CeF$_3$ with a scan rate of 150 mV/s

Fig.5a shows the cyclic voltammogram curves of molybdenum electrode recorded in molten CeF_3-LiF-BaF_2 containing 2 wt% CeO_2. As shown in the figure, a reduction current peak D is formed at about –1.0 V (vs. C/CO_x), which can be attributed to the electrochemical reduction of cerium-oxygen-fluorine ions generated by the reaction between CeO_2 and CeF_3 as discussed above.

In order to further confirm the reduction reaction occurred within the potential range of current peak D, cyclic voltammogram experiment was performed by narrowing the scanning potential range from –0.5 V to –1.25 V (vs. C/CO_x), as shown in Fig.5b. It is worth noting that a reoxidation peak D′ is visible upon reversing the potential scan, indicating that the electrochemical reduction of cerium-oxygen-fluorine ions is reversible. As for the absence of current peak D′ in Fig.5a, it may be due to the overlap of the reoxidation current at C′ and D′, because the final reduction product of both CeF_3 and CeOF is metal cerium.

According to previous studies on cyclic voltammograms, the number of exchanged electrons can be deduced by calculating the slope ($k=RT/n$F) of the curves of potential E vs. ln[$(i_p-i)/i_p$]. For the reduction peak D, the linear plot of potential E vs. ln[$(i_p-i)/i_p$] is shown in Fig.6. From the slope (k=0.0336), the exchanged electron number of the reduction of cerium ions is approximately equal to 3. So it can be concluded that the Ce(III) in CeOF is electro-reduced to metal cerium directly.

2.3 Chronoamperometry

In order to confirm the rate-limiting step of the electro-deposition reaction of cerium, chronoamperometric experiments were carried out on molybdenum electrode. Fig.7 shows the chronoamperograms obtained at different applied potentials varied from –0.9 V to –1.5 V (vs. C/CO_x). It is observed that currents are fairly low during the potentiostatic polarization between –0.9 V (vs. C/CO_x) and –1.0 V (vs. C/CO_x), indicating that no reduction occurs. By increasing the potential to –1.1 V (vs. C/CO_x), an increase in current is observed and current step S1 appears. Similarly, current step S2 is observed when the potential increases to –1.5 V (vs. C/CO_x). Supported by the results of cyclic voltammetry, it can be concluded that the step change S1 is attributed to the reduction of cerium ions formed by CeOF and the step change S2 is attributed to the reduction of Ce(III) formed by CeF_3.

In addition, according to the Cottrell equation[24], the current I_t is correlated with the function of time ($t^{-1/2}$) for diffusion controlled step:

$$I_t = nFAD^{1/2}C/(\pi^{1/2}t^{1/2}) \quad (3)$$

where n is the number of exchanged electrons, F is the faraday constant (96485 C), A is the surface area of the electrode in cm^2, D is the diffusion coefficient in $cm^2 \cdot s^{-1}$, C is the bulk concentration of reducible ions in $mol \cdot cm^{-3}$, and t is the polarization time.

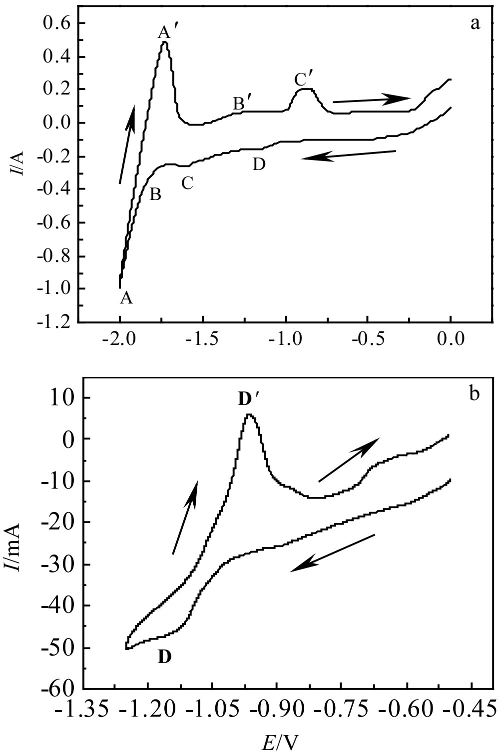

Fig.5 Cyclic voltammetry curves of molybdenum electrode in molten CeF_3-LiF-BaF_2-2wt% CeO_2 with a scan rate of 150 mV/s: (a) –2.0~0.0 V and (b) –0.5~ –1.25 V

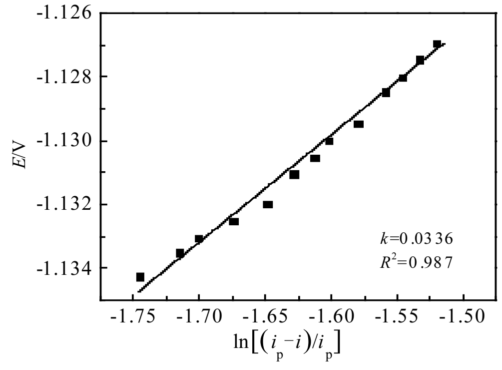

Fig.6 Linear correlation between potential E and ln[$(i_p-i)/i_p$]

The Cottrell equation indicates the linear relationship between current I_t and inverse $t^{1/2}$ caused by the depletion of electro-active species near the working electrode surface. Fig.8 shows the plot of current I_t vs. $t^{-1/2}$ at –1.1 V (vs. C/CO_x). It can be seen that the current increases linearly with the increase of $t^{-1/2}$, demonstrating that the electro-reduction process is a diffusion controlled step and this result is in agreement with the theory proposed by Wang et al[25].

2.4 Constant potential electrolysis

According to the results of electrochemistry tests, CeO_2

can dissolve into the molten CeF_3-LiF-BaF_2 in the form of CeOF which can be reduced at a relatively low potential, about –1.0 V (vs. C/CO_x). In order to further confirm the electrode reaction at this potential, constant potential electrolysis was carried out at –1.25 V (vs. C/CO_x) for 2 h. After potentiostatic electrolysis, the washed and dried product was analyzed by XRD. As shown in Fig.9, the obtained cathode product is mainly cerium, indicating that CeOF was reduced to metal cerium by direct electrochemical reduction reaction.

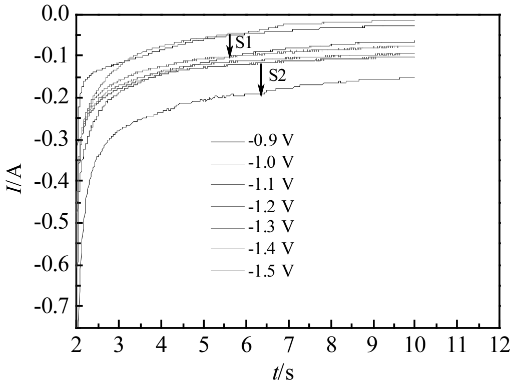

Fig.7 Constant potential step curve of CeF_3-LiF-BaF_2-2wt% CeO_2 molten salts on molybdenum electrode

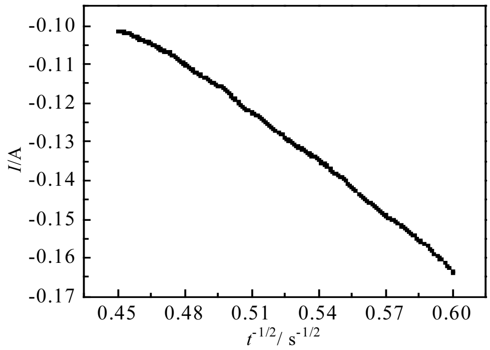

Fig.8 Relation between I and $t^{-1/2}$ constructed from the curve at –1.1 V (vs. C/CO_x) in Fig.7

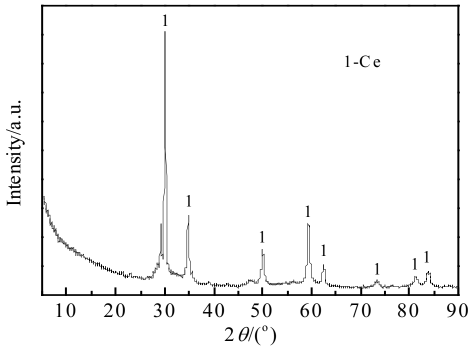

Fig.9 XRD pattern of product obtained by potentiostatic electrolysis at –1.25 V (vs. C/CO_x) for 1 h

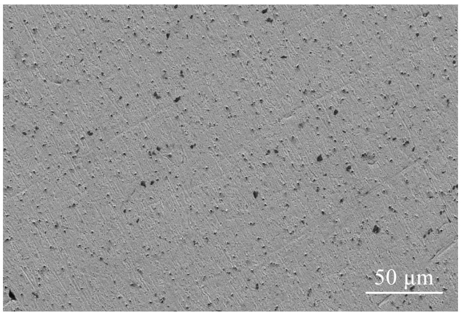

Fig.10 SEM image of potentiostatic electrolysis product obtained at –1.25 V (vs. C/CO_x)

The SEM image of the product obtained by potentiostatic electrolysis experiment is exhibited in Fig.10. The product shows metal luster and has a dense microstructure. The content of cerium was 99.38 wt%~99.81 wt%, tested by decrement method.

3 Conclusions

1) CeO_2 can dissolve in molten CeF_3-LiF-BaF_2 in the form of CeOF, by reacting with CeF_3.

2) Cerium oxyfluorides can be directly electro-reduced to metal cerium with a purity of 99.38 wt%~99.81 wt% at about –1.0 V (vs. C/CO_x).

3) The electrochemical reduction process is one-step process involving the three electron exchanges and controlled by diffusion.

References

1 Li Q L, Xia T D, Lan Y F *et al. Journal of Alloys and Compounds*[J], 2013, 562(15): 25

2 Vijayan V, Prabhu K N. *Canadian Metallurgical Quarterly*[J], 2014, 54(1): 66

3 Liu S Q, Cui C X, Wang X *et al. Metals*[J], 2017, 7(6): 204

4 Yu Xuan, Zhang Zhihao, Xie Jianxin. *Acta Metallurgica Sinica*[J], 2017, 53(8): 927 (in Chinese)

5 Rusman N A A, Dahari M. *International Journal of Hydrogen Energy*[J], 2016, 41(28): 12 108

6 Zhu M G, Li W, Wang J D *et al. IEEE Transactions on Magnetics*[J], 2014, 50(1): 1

7 Liu R M, Zhu D M, Jia L Y *et al. Ferroelectrics*[J], 2018, 522(1): 122

8 Pathak A K, Khan M, Gschneidner K A *et al. Advanced Materials*[J], 2015, 27(16): 2663

9 Wheeler D W, Zekonyte J, Wood R J K. *Materials Science and Engineering A*[J], 2013, 578(1): 294

10 Liu X P, Jiang L J, Li Z N *et al. Journal of Alloys and Compounds*[J], 2009, 47(1-2): L36

11 Singh G, Thomas V, Tiwari V S *et al. Ceramics International*[J], 2017, 43(12): 9032

12 Naumov A V. *Russian Journal of Non-Ferrous Metals*[J], 2008, 49(1): 14

13 Zhang Meng, Li Yunna, Han Wei *et al. Rare Metal Materials and Engineering*[J], 2016, 45(8): 1956

14 Wang C S, Liu Y, He H *et al. Journal of Rare Earths*[J], 2013, 31(4): 405

15 Qi X, Zhu H M. *Rare Metals*[J], 2005, 24(1): 8

16 Constantin V, Popescu A, Olteanu M. *Journal of Rare Earths*[J], 2010, 28(3): 428

17 Lin R S, Ye G A, He H *et al. Journal of Rare Earths*[J], 2012, 30(2): 151

18 Xu G X. *Rare Earths*[M]. Beijing: Metallurgical Industry Press, 1995, 8 (in Chinese)

19 Stefanidaki E, Hasiotis C, Kontoyannis C. *Electrochimica Acta*[J], 2001, 46(17): 2665

20 Chen Z, She C F, Zheng H Y *et al. Electrochimica Acta*[J], 2018, 261: 289

21 Gao Y, Shi Y K, Liu X L *et al. Electrochimica Acta*[J], 2016, 190: 208

22 Massot L, Chamelot P, Taxil P. *Electrochimica Acta*[J], 2005, 50(28): 5510

23 Huang C, Liu X, Gao Y *et al. Faraday Discussions*[J], 2016, 190: 339

24 Bard A J, Faulkner L R. *Electrochemical Methods, Fundamentals and Application*[M]. New York: John Wiley & Sons Inc, 2001

25 Wang X, Liao C F, Jiao Y F *et al. Journal of Rare Earths*[J], 2018, 36(3): 324

CeO_2在CeF_3-LiF-BaF_2熔盐中的溶解过程及电化学行为

李斌川[1]，李师居[2]，孔亚鹏[1]，陈建设[1]，刘奎仁[1]，韩 庆[1]

(1. 东北大学 多金属共生矿生态化冶金教育部重点实验室，辽宁 沈阳 110819)

(2. 东北大学 材料电磁过程研究教育部重点实验室，辽宁 沈阳 110819)

摘　要：研究了CeO_2在CeF_3-LiF-BaF_2熔盐中的溶解机理，并采用钼金属电极研究了Ce(III)在CeF_3-LiF-BaF_2熔盐中的电化学行为。通过循环伏安曲线、计时电流法、恒电位电解法研究了Ce(III)的电解还原机理，并采用XRD、SEM、EDS对溶解反应产物和电解产物进行了物相、成分和微观组织分析。结果表明：CeO_2可通过与CeF_3反应生成CeOF进而溶解于CeF_3-LiF-BaF_2熔盐中，CeOF可直接被电解还原生成纯度为99.38%~99.81%的金属Ce。Ce(III)在Mo电极上的电化学反应是一个单步的三电子可逆过程，反应受扩散控制。

关键词：铈；氟化物熔盐；CeF_3-LiF-BaF_2；CeO_2；电沉积

作者简介：李斌川，男，1976年生，博士，讲师，东北大学冶金学院，辽宁 沈阳 110819，电话：024-83686997，E-mail: libc@smm.neu.edu.cn